*Supplement of*

# A new method of resolving annual precipitation for the past millennia from Tibetan ice cores

Wangbin Zhang et al.

*Correspondence to:* Shugui Hou (shugui@nju.edu.cn; shuguihou@sjtu.edu.cn)

- Figures S1 to S8.
- Tables S1

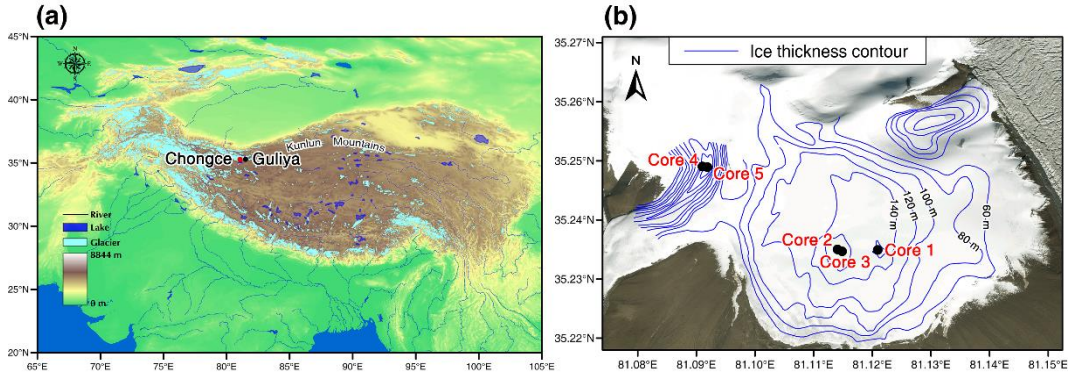


**Figure S1.** (a) Map showing the drilling sites of Chongce (red solid dot) and Guliya ice cores (black solid dot). The topographic data were extracted from the ETOPO1 elevations global data, available from National Oceanic and Atmospheric Administration at http://www.ngdc.noaa.gov/mgg/global/global.html. (b) Remote sensing image showing Chongce ice cap and the locations of ice core drilling sites. Blue contour lines indicate ice thickness.

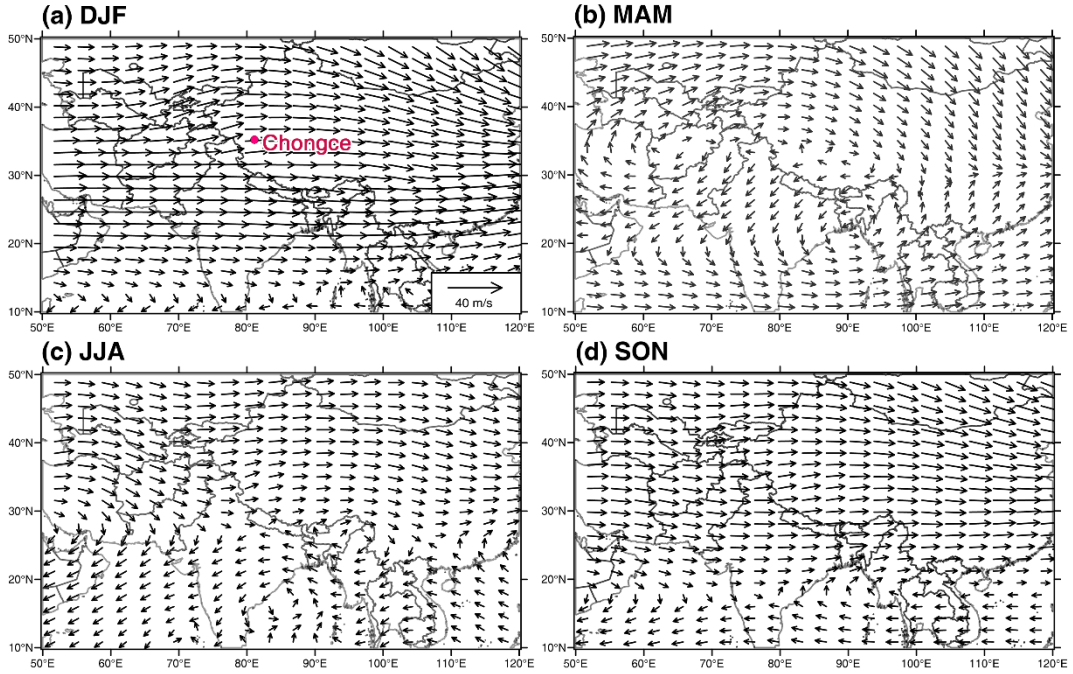


**Figure S2.** Seasonally averaged horizontal wind patterns at 500 hPa over the Tibetan Plateau and its vicinity. Wind speed data are from the ERA 5 (available at: https://www.ecmwf.int/).

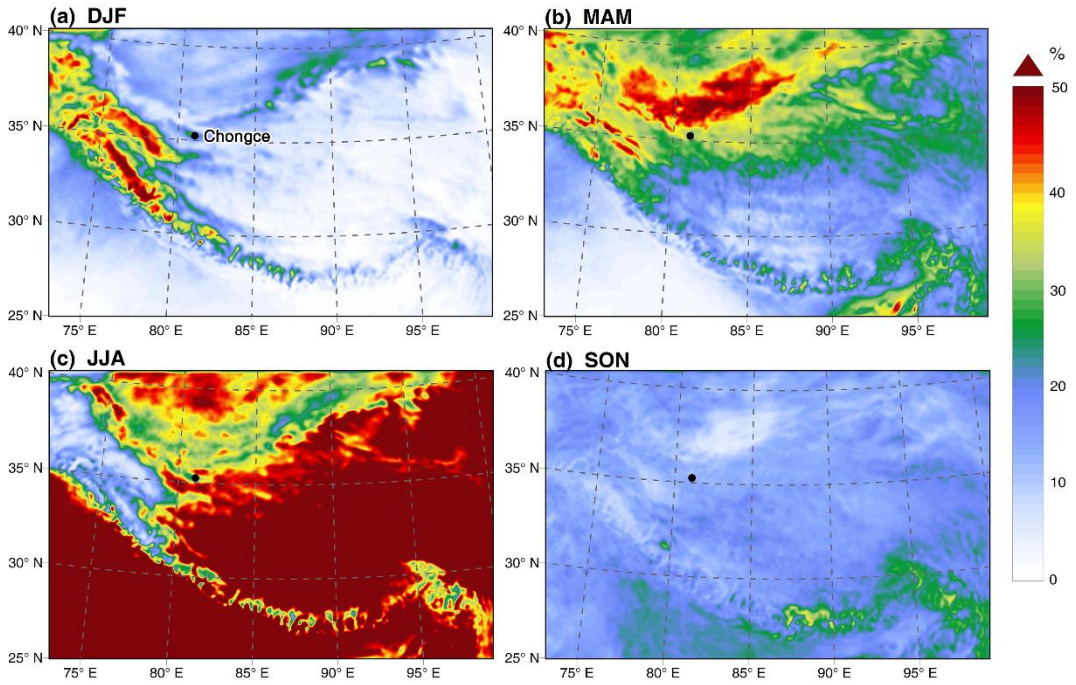


**Figure S3.** Seasonal precipitation regimes on the Tibetan Plateau. Percentage of annual precipitation in winter (DJF) (a), spring (MAM) (b), summer (JJA) (c), and fall (SON) (d), calculated by the High Asia Refined analysis dataset (2001-2013 AD) with spatial resolution of 10 km (Maussion et al., 2014).

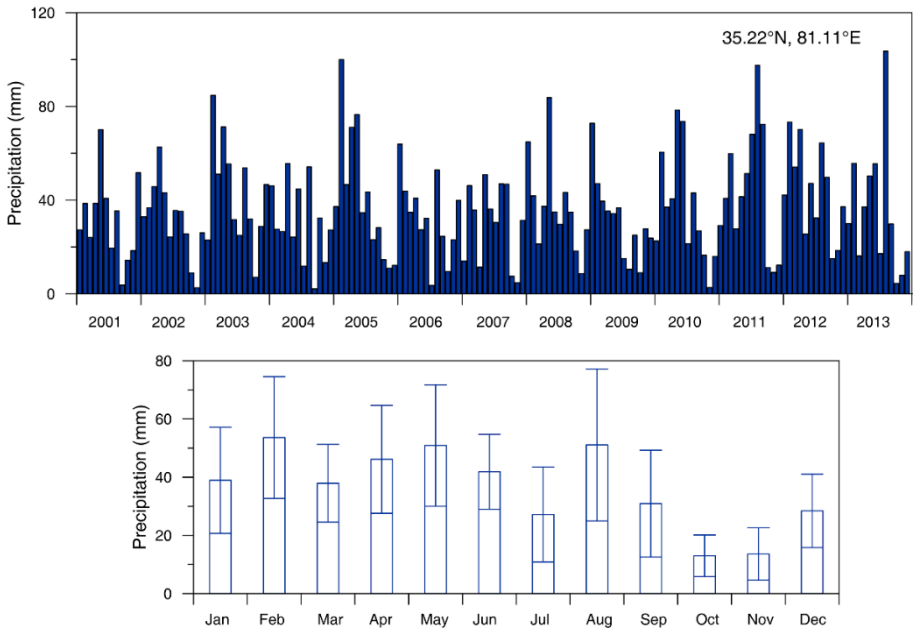


**Figure S4.** The seasonal precipitation distribution in the vicinity of the Chongce ice cap, as shown by High Asia Refined monthly data from 2001 A.D. to 2013 A.D. (top) and by the monthly climatology for this period (bottom) (Maussion et al., 2014). Approximately 27.8% of annual precipitation falls from June to August, 13.3% from September to November, 27.9% from December to February, and 31.1% from March to May.

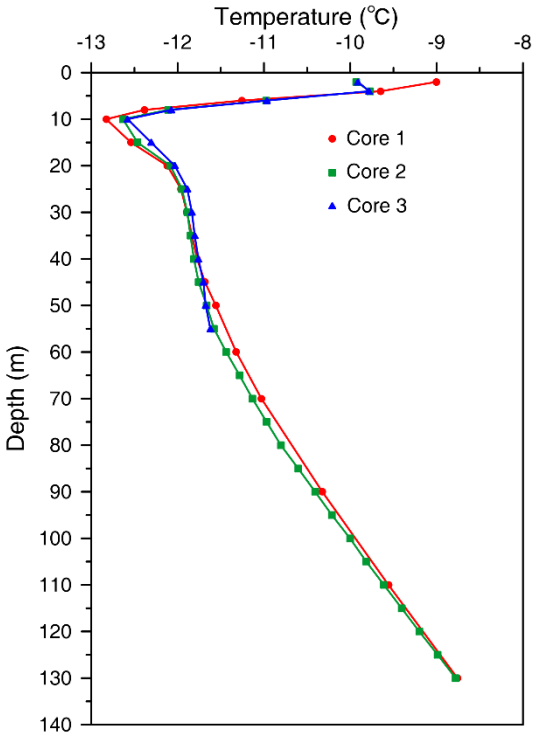


**Figure S5:** Borehole temperature profiles of the Chongce Core 1, Core 2 and Core 3.

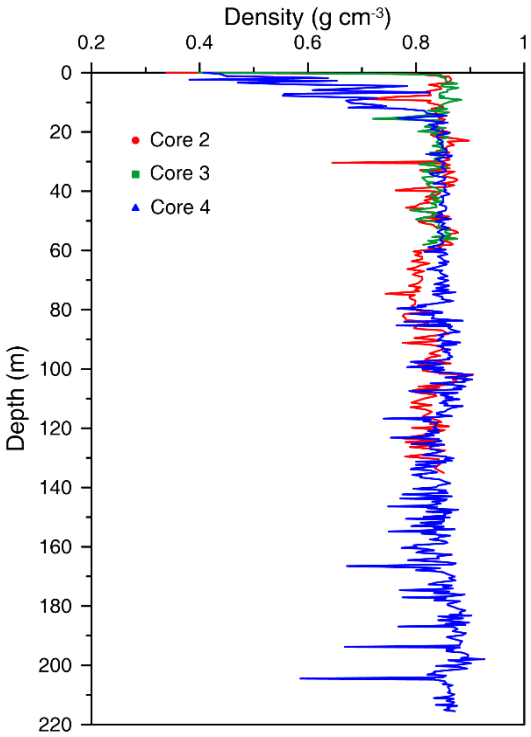


**Figure S6.** Density profiles of the Chongce Core 2, Core 3 and Core 4.

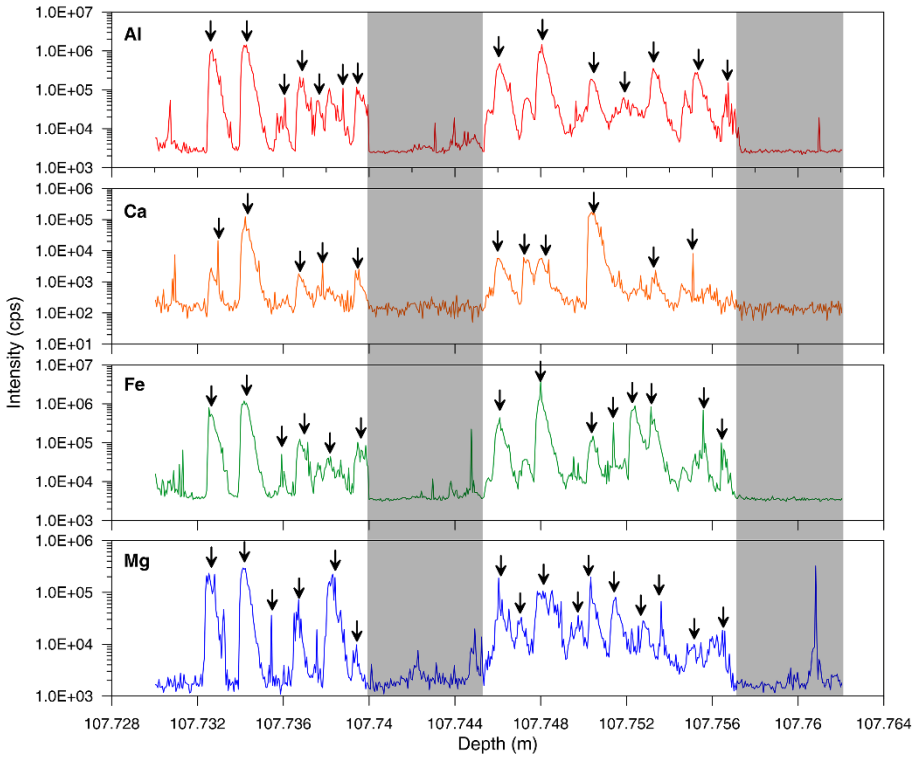


140

**Figure S7.** Annual layer counting example taken from Section II, an ~4 cm section shown for Al (red), Ca (orange), Fe (green), and Mg (blue). Black arrows show multiple individual peaks, which can be considered as sub-annual dust events during winter and spring. Grey bars show 'synchronous' trough in all the four elements (Al, Ca, Fe, and Mg) measured, which can be considered as summer snow layers with weak dust deposition.

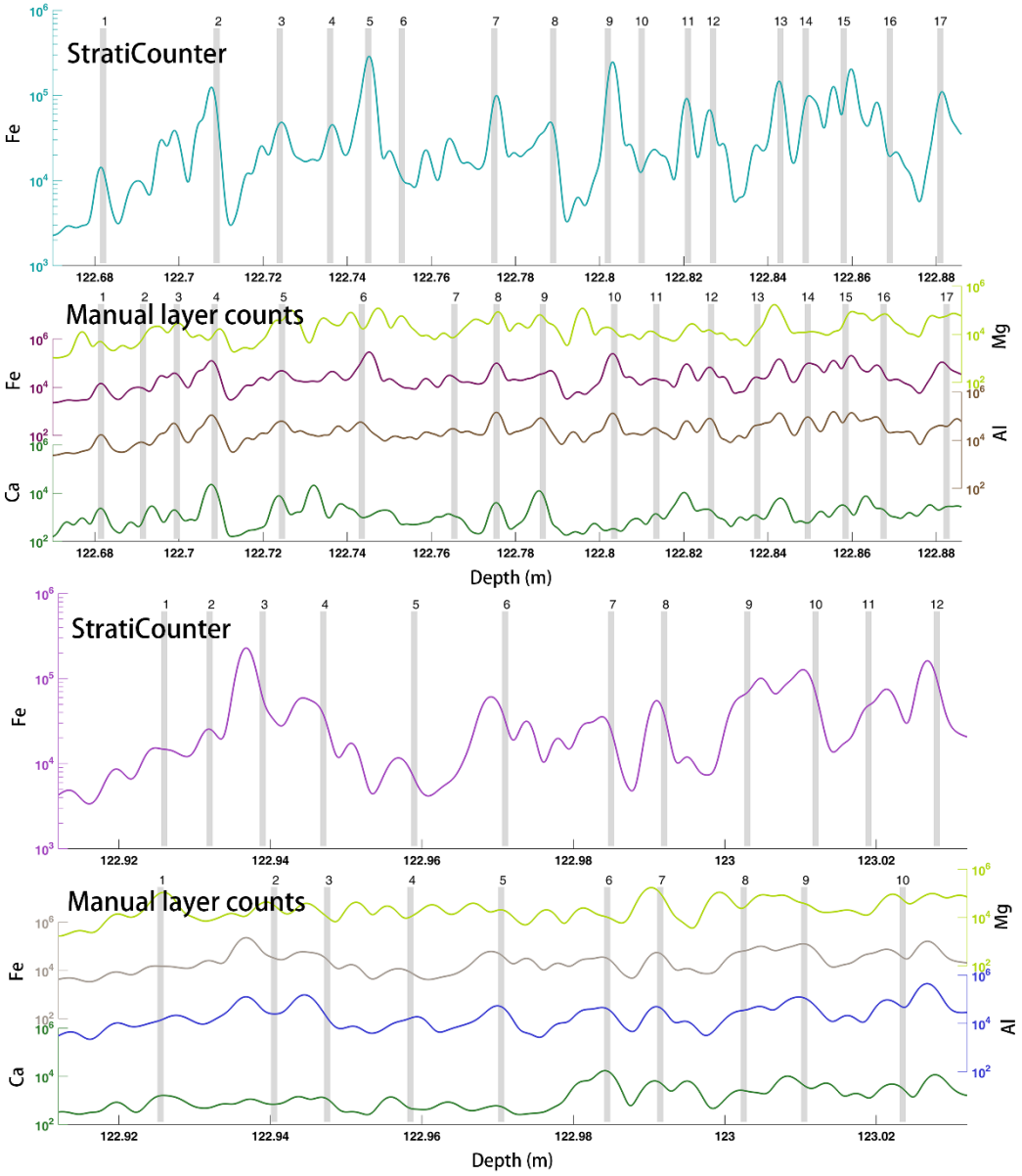


**Figure S8.** Comparisons between StratiCounter and manual annual-layer counts (grey bars).

**Table S1.** The $^{14}C$ dating of 135.81 m Chongce ice core. Absolute uncertainties are given as 1$\sigma$ range.

| Sample # | Depth (m) | Mass (g) | WIOC (μg) | $F^{14}C$ | $^{14}C$ age (ka B.P.) | Cal. age (ka B.P.) |
|---|---|---|---|---|---|---|
| CC-1 | 79.46-80.21 | 307.7 | 20.3 ± 1.2 | 0.81 ± 0.01 | 1.679 ± 0.078 | 1.445-1.704 |
| CC-2 | 88.82-89.56 | 302.9 | 24.3 ± 1.4 | 0.80 ± 0.01 | 1.831 ± 0.138 | 1.572-1.921 |
| CC-3 | 99.44-100.10 | 304.6 | 13.8 ± 0.9 | 0.68 ± 0.01 | 3.133 ± 0.161 | 3.157-3.560 |
| CC-4 | 110.58-111.35 | 342.6 | 24.9 ± 1.4 | 0.78 ± 0.01 | 2.037 ± 0.142 | 1.827-2.296 |
| CC-5 | 116.62-117.43 | 330.9 | 9.1 ± 0.7 | 0.69 ± 0.01 | 3.012 ± 0.164 | 2.978-3.377 |
| CC-6 | 122.64-123.36 | 338.6 | 17.6 ± 1.1 | 0.69 ± 0.01 | 2.944 ± 0.157 | 2.892-3.331 |
| CC-7 | 131.41-132.10 | 324.6 | 22.6 ± 1.3 | 0.59 ± 0.01 | 4.228 ± 0.176 | 4.451-5.036 |
| CC-8 | 132.65-133.51 | 392.7 | 23.6 ± 1.4 | 0.60 ± 0.01 | 4.169 ± 0.175 | 4.424-4.951 |
| CC-9 | 134.31-135.03 | 292.4 | 23.0 ± 1.4 | 0.51 ± 0.01 | 5.466 ± 0.201 | 5.997-6.443 |